Quantitative Analysis of Polymer Dilation during Sorption Using FTIR-ATR Spectroscopy

Marco Giacinti Baschetti,[†] Enrico Piccinini,[†] Timothy A. Barbari,*[,‡] and Giulio C. Sarti[†]

Dip. Ingegneria Chimica, Mineraria e delle Tecnologie Ambientali, Università degli Studi di Bologna, viale Risorgimento 2 40136 Bologna Italy, and Department of Chemical Engineering, University of Maryland, College Park, Maryland 20742

Received April 25, 2003; Revised Manuscript Received September 24, 2003

ABSTRACT: The dilation of polycarbonate (PC), poly(vinyl acetate) (PVAc), and poly(ether urethane) (PEUT), induced by acetonitrile sorption at 40 °C, was studied using FTIR-ATR spectroscopy. Results compared well to those obtained through direct observation of volumetric changes using a CCD camera. Polymer dilation and penetrant sorption kinetics were monitored simultaneously with the spectroscopic technique, allowing further mechanistic insight into these processes. For the rubbery polymers (PVAc and PEUT), a linear relationship exists between time-evolved dilation and sorption, indicating that chain relaxation is fast relative to the diffusion process. However, for the glassy polymer (PC), there is a lag in dilation relative to sorption, suggesting that the nonequilibrium microvoids are filled before significant dilation occurs in the polymer. Model predictions of the extent of dilation, using the lattice fluid model for PVAc and PEUT and the nonequilibrium lattice fluid model for PC, overestimate the experimental data, particularly for PC. The large deviation for PC is due to the extreme sensitivity of the NELF model to polymer density, which is used to reflect the nonequilibrium nature of the glassy polymer and is strongly history dependent.

Introduction

The use of Fourier transform infrared, attenuated total reflectance (FTIR-ATR) spectroscopy in polymer science has grown in recent years, not only in the classical areas of surface characterization[1−3] and depth profiling[4,5] but also in new applications, such as the study of transport properties of polymeric materials. A number of studies on polymer−polymer interdiffusion[6−8] and on diffusion of small molecules in polymeric materials[9−14] using FTIR-ATR spectroscopy showed the potential of this technique to go beyond the simple determination of the diffusion coefficients of the species involved. One of the primary features of infrared spectroscopy, namely the effect of local environment on the location of infrared bands, allows a deeper inspection of the diffusion process at a molecular level, which is particularly important when the transport process itself is accompanied by reaction[15,16] or association and solvation,[17−20] which can affect the behavior of the different components.

The use of the FTIR-ATR technique for the study of polymer−penetrant systems, as well as for multicomponent diffusion,[21] has been considered and explained in previous studies. In the present study, the attention is focused on another interesting application of FTIR-ATR spectroscopy in the analysis of the diffusion process: the in situ monitoring of polymer swelling. The analysis of the IR spectra of a given penetrant−polymer system allows for the determination of the transport properties of the penetrant from IR absorbance peaks associated with the penetrant and can also offer information on polymer swelling through changes in the IR absorbance peaks of the polymer. Knowledge of the volumetric behavior of the system during diffusion is critical for a complete characterization of the transport properties of a given polymer−penetrant pair and is important for both theoretical and applied research.

From studies of diffusion in glassy polymers, it is well-known that the mass transport behavior of a given polymer−penetrant system is related to the rate of penetrant diffusion in the polymeric matrix and the rate of relaxation of the polymer chains during sorption. Historically, the mass transport properties of polymers were important to membrane separation processes and packaging applications, but the recent development of polymer-based electronic sensors for environmental control has made the knowledge of polymer swelling behavior increasingly important. A critical role in these sensors is played by the thickness of the polymeric layer.[22−24]

Prior to this study, the measurement of polymer swelling during sorption of a light gas or vapor has usually been carried out separately from the diffusion experiment, increasing the potential for uncertainties that can affect the results, particularly for a glassy polymer, whose behavior depends strongly on its history. This drawback can be overcome with the use of FTIR-ATR spectroscopy, which allows monitoring, simultaneously, both the diffusion of the penetrant and the dilation of the matrix. While several authors have already pointed out the capability of the ATR technique in monitoring polymer swelling and have reported some results,[25,26] very few attempts have been made, to our knowledge, to study the relation between diffusion and swelling through this technique quantitatively.

[†] Università degli Studi di Bologna.
[‡] University of Maryland.
* To whom correspondence should be addressed: phone 301-405-2983; fax 301-405-0523; e-mail barbari@eng.umd.edu.

10.1021/ma0302457 CCC: $25.00
Published on Web 11/14/2003

Table 1. Physical Properties of Polymers and the Penentrant Used in This Study

polymers	suppliers	mol wt (M_w)	density ρ (g/cm^3)	glass transition (T_g) (°C)	refractive index (n)
PEUT	Thermedics		1.04	−75	1.487
PC (Maryland)	Scientific Polymer Products, Inc.	≈60 000	1.200	150	1.586
PC (Bologna)	Aldrich	≈64 000	1.200	149	1.586
PVAc (Maryland)	Scientific Polymer Products, Inc.	≈260 000	1.18	30	1.467
PVAc (Bologna)	Aldrich	≈167 000	1.191	30	N/A
CH_3CN (penetrant)	Aldrich	41	0.786	82 (T_b)	1.344

In this work, an evaluation of penetrant-induced dilation in different polymeric materials using the FTIR-ATR technique is considered and analyzed. The reliability of the experimental results was tested by comparing the spectroscopic measurements with those obtained directly through the use of a CCD camera. A prediction of the extent of swelling, which can be obtained from suitable thermodynamic models and solubility data, is also introduced to provide further contributions to the discussion. In particular, the diffusion of acetonitrile in polycarbonate (PC), poly(vinyl acetate) (PVAc), and poly(ether urethane) (PEUT) at 40 °C was studied. The choice of these materials was made considering their potential application in electronic sensors and on the molecular features that make them suitable for spectroscopic analysis. PC, PVAc, and PEUT all have, in their repeat units, a carbonyl group that can be easily monitored during sorption to determine the dilation. The choice of acetonitrile was made to facilitate spectroscopic observations since the nitrile group in this penetrant does not interfere with any part of the polymer spectrum.

Experimental Section

The experiments for this study were carried out partially in the laboratories of the Department of Chemical Engineering at Johns Hopkins University, Baltimore, MD, by Giacinti Baschetti and Barbari (now at the University of Maryland, College Park, MD) and partially in those of the Dipartimento di Ingegneria Chimica, Mineraria e Delle Tecnologie Ambientali at the University of Bologna, Italy, by Giacinti Baschetti, Piccinini, and Sarti. The experimental apparatuses used in the two laboratories were similar and both composed of a spectrometer coupled to a quartz spring system for sorption and diffusion measurements. A more detailed description of the apparatus used in Maryland can be found in the literature[13] while a simple schematic of the one in Bologna is shown in Figure 1. The spectrometers used were a Mattson Research Series 1 (Maryland) and a Nicolet Avatar (Bologna), and both had MCT detectors to improve measurement accuracy. The quartz springs for both were purchased from Ruska Instruments (Houston, TX). The apparatus used in Bologna also included a special cell with glass windows for the measurement of dilation with a CCD camera.

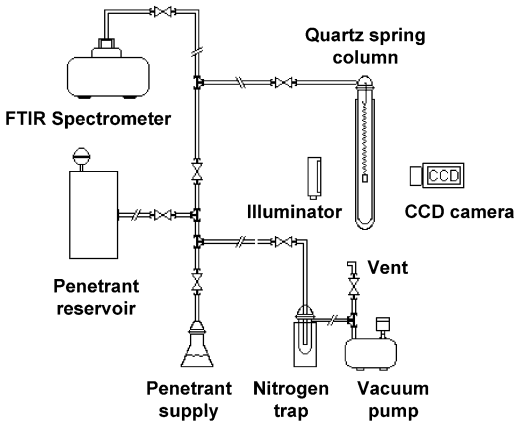

Figure 1. Schematic of the experimental apparatus used in the laboratories in Bologna, Italy.

The polymers used in the two laboratories and their physical properties are reported in Table 1. It is important to note that the samples of PC and PVAc used in Bologna did not show significant differences from those used in Maryland, in either sorption or dilation, when the same protocols were followed for sample preparation. The samples were prepared via solvent evaporation starting from solutions of PVAc (5 wt %) in acetone and PC (4 wt %) or PEUT (10 wt %) in dichloromethane.

The films for the gravimetric experiments were obtained by casting an adequate amount of the solution on a clean surface (glass, steel, or aluminum) and allowing the solvent to evaporate, whereas in the case of the FTIR-ATR experiments, the polymer was cast directly onto 45° ATR crystals. The films were left for 24 h in a clean hood and then placed in a vacuum oven, a few degrees below T_g, for at least 48 h. This protocol ensured the removal of residual solvent and, for the ATR sample, intimate contact between the polymeric film and the crystal.

The FTIR-ATR experiments were conducted by mounting the crystal in the ATR cell as shown in Figure 2 and measuring the time evolution of the penetrant and polymer peaks. Specifically, the acetonitrile content was determined from the two bands at 2251 and 2292 cm^{-1}, which are related respectively to the nitrile group (C≡N) stretching and to a combination of CH_3 bending and C−C stretching modes.[27,28] Polymer swelling was monitored through the carbonyl (C═O) group stretching band located at 1734, 1770, and 1718 cm^{-1} in PVAc, PC, and PEUT, respectively. Typical spectra are shown in Figure 3 for the three polymers with sorbed penetrant. For the ATR experiments, it should be noted that different crystals were used for the different polymers; in particular, silicon (refractive index 3.42) for PC and PVAc and zinc selenide (refractive index 2.42) for PEUT. These choices were made because of the different intensities of the carbonyl absorption peak in the three polymers; PC and PVAc had very strong peaks that saturate the detector if used with a ZnSe crystal, preventing a quantitative analysis of dilation. PVAc and PC spectra were collected by co-adding 32 scans with a resolution of 4 cm^{-1}, but since experiments in PEUT are extremely fast, the collection time was reduced for this polymer, co-adding only eight scans per spectrum with the same resolution. The lower signal-to-noise ratio obtained with PEUT was partially compensated by the higher signal that can be obtained with ZnSe crystals.

In the gravimetric experiments, the polymeric film was detached from the substrate onto which it was previously cast and hung directly on the quartz spring. The spring extension was then monitored and used to calculate the mass uptake. The evaluation of swelling was achieved by mounting the free samples on a fixed frame to prevent bending and rigid deformation of the polymers and monitoring the dilation through a CCD camera. Image processing software was used to obtain data on polymer dilation during sorption. The thickness of the samples was measured after each ATR experiment using a micrometer with a precision of ±1 μm; the average thickness of the different films was roughly 20 μm for PC, 30 μm for PVAc, and 80 μm for PEUT. Differences between the various samples of each polymer never exceeded

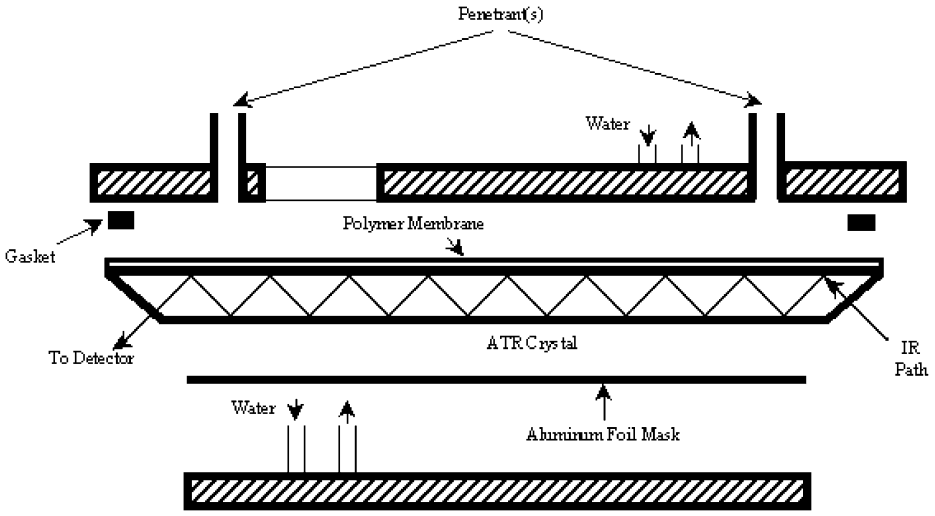

Figure 2. ATR cell for diffusion in polymer films. Water inlet and outlet ports are for temperature control.

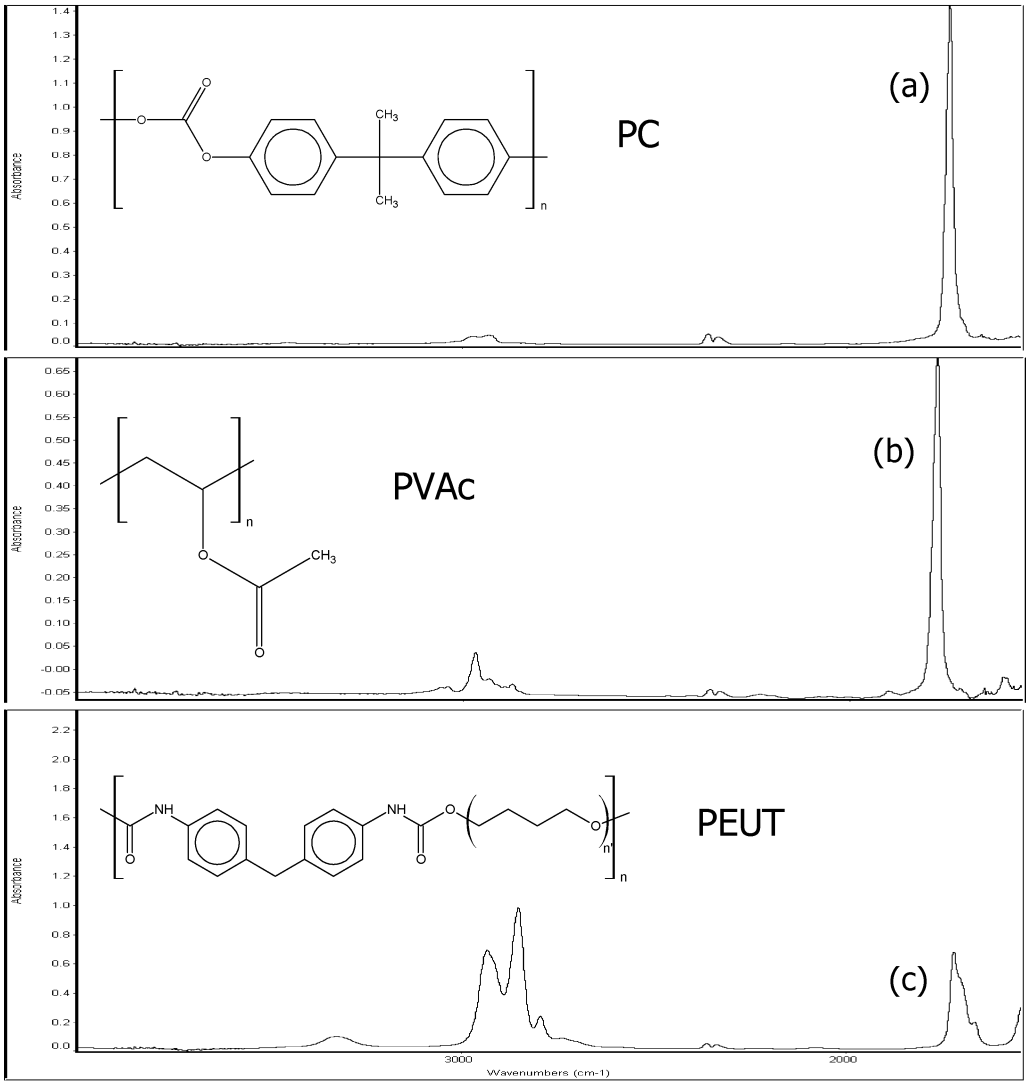

Figure 3. IR spectra for PC (top), PVAc (middle), and PEUT (bottom). Bands located at 1734 (a), 1770 (b), and 1718 cm^{-1} (c) were used for determining polymer swelling.

25%. As a rule, the films used for gravimetric and dilation experiments were approximately 2 times thicker than those used in the spectroscopy experiments to obtain similar diffusion times; however, no relevant influence of specimen thickness on the experimental results was observed during this study.

Background

Diffusion Coefficient Evaluation. For a one-dimensional diffusion process, the combination of Fick's law and the continuity equation for the diffusing component gives the following equation:

$$\frac{\partial C}{\partial t} = D_{\text{eff}} \frac{\partial^2 C}{\partial z^2} \tag{1}$$

where C is the concentration of the penetrant, D_{eff} is the effective diffusion coefficient, treated here as a concentration-averaged constant at a particular penetrant activity, and t and z are time and space coordinates, respectively. An appropriate set of boundary and initial conditions describing both the ATR and spring experiments is the following:

$$\begin{aligned} C &= C_0 \quad \text{at} \quad 0 < z < L \text{ and } t = 0 \\ \frac{\partial C}{\partial z} &= 0 \quad \text{at} \quad z = 0 \text{ and } t \geq 0 \\ C &= C_{\text{eq}} \quad \text{at} \quad z = L \text{ and } t \geq 0 \end{aligned} \tag{2}$$

where C_{eq} is the concentration in the film when equilibrium is attained and L is the thickness (ATR experiments) or half thickness (spring apparatus) of the film; the z-axis is normal to the surface at zero flux, with an opposite direction with respect to that of the diffusive flux.

One solution to eq 1 with these initial and boundary conditions is[29]

$$\frac{C(t,z) - C_0}{C_{\text{eq}} - C_0} = 1 - \frac{4}{\pi} \sum_{n=0}^{\infty} \frac{(-1)^n}{2n+1} \times \exp\left[\frac{-D_{\text{eff}}(2n+1)^2\pi^2 t}{4L^2}\right] \cos\left[\frac{(2n+1)\pi z}{2L}\right] \tag{3}$$

Equation 3 gives the concentration profile in the film during diffusion, which can be related to the mass uptake in the gravimetric experiments through simple integration along the space coordinate over the total sample thickness. The final result can be written as

$$\frac{m(t) - m_0}{m_{\text{eq}} - m_0} = 1 - \frac{8}{\pi^2} \sum_{n=0}^{\infty} \frac{1}{(2n+1)^2} \times \exp\left[\frac{-(2n+1)\pi^2 D_{\text{eff}} t}{4L^2}\right] \tag{4}$$

where m_0 and m_{eq} are the initial and equilibrium mass uptakes, respectively, and $m(t)$ is the mass uptake at time, t. For the ATR experiments, eq 3 has to be related to the IR absorbance data through the use of the ATR differential form of the Beer−Lambert law:[37]

$$A = \int_0^L \epsilon^* C \exp\left(-2\frac{z}{d_p}\right) dz \tag{5}$$

In eq 5, valid under the condition of weak IR absorption, the molar extinction coefficient, ϵ^*, can be considered constant, A is the ATR integrated absorbance, and d_p is the penetration depth defined as

$$d_p = \frac{\lambda}{2\pi n_1 \sqrt{\sin^2\theta - (n_2/n_1)^2}} \tag{6}$$

where n_1 and n_2 are the refractive indices respectively of the polymer and of the ATR crystal, θ is the angle of incidence, and λ is the wavelength of the absorbed light. Combining eqs 3 and 5, infrared absorbance depends on time through the following relation[11]

$$\frac{A(t) - A_0}{A_{\text{eq}} - A_0} = 1 - \frac{8}{\pi d_p\left[1 - \exp\left(-2\frac{L}{d_p}\right)\right]} \times \sum_{n=0}^{\infty} \left[\frac{\exp(g)\left[f \exp\left(-2\frac{L}{d_p}\right) + (-1)^n\left(\frac{2}{d_p}\right)\right]}{(2n+1)\left(\frac{4}{{d_p}^2} + f^2\right)}\right] \tag{7}$$

$$g = \frac{-D_{\text{eff}}(2n+1)^2\pi^2 t}{4L^2}$$

$$f = \frac{(2n+1)\pi}{2L}$$

where A_0 and A_{eq} are the initial and equilibrium IR absorbances, respectively, and $A(t)$ is the absorbance at time, t. Equations 4 and 7 allow for the determination of the effective diffusion coefficient through a least-squares regression of the sorption kinetics data. Given that the IR bands associated with acetonitrile can be considered to be weak absorbers and that the acetonitrile concentrations observed in this work are low (less than 10 wt %), the assumptions used to derive eq 7 are reasonable for the systems studied here.

Dilation Measurements and Analysis. The dilation of the polymeric matrix during the sorption process was measured independently through either direct observation of the samples with a CCD camera or monitoring characteristic IR peaks in the polymer during the diffusion experiments with the ATR technique. When the polymer swells during penetrant sorption, the concentration of polymer chains in the region probed by the infrared beam decreases, lowering the number of polymer functional groups that can interact with the IR beam and absorb energy. A decrease in the integrated absorbance of the polymer peaks, shown in Figure 4, is the result of such a process and can be used to evaluate the matrix volume change upon mixing. A comparison between the two techniques was considered, since no previous experimental evidence has been presented that correlates, in a quantitative way, the decrease in polymer peak integrated absorbance with direct dilation data. The problem is not trivial considering that (a) the concentration of IR-absorbing functional groups in the polymer does not normally allow one to consider the system to be dilute and the constancy of the molar extinction coefficients associated with the polymer in the Beer−Lambert law may not be assured; (b) IR dispersion phenomena, associated with changes in the real part of the refractive

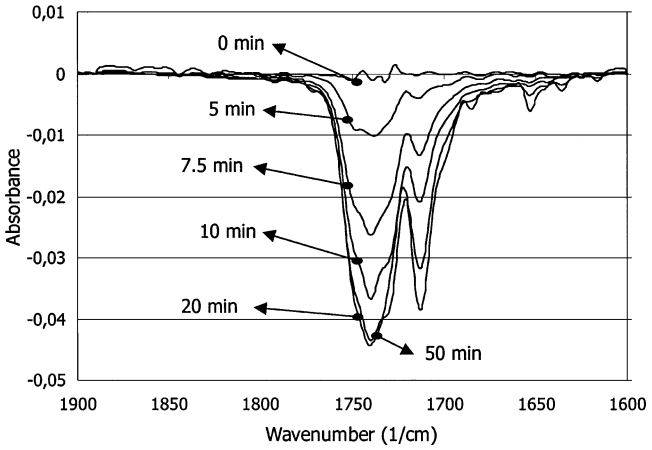

Figure 4. IR absorbance of polymer characteristic peaks (PVAc) during acetonitrile diffusion. Each time point represents the difference from the initial value, A_0.

index in strongly IR-absorbing systems, can affect the ATR signal and the calculated absorbance value;[30] and (c) misleading results can be obtained with a nonhomogeneous sample as a consequence of the film casting procedure or detachment of the film from the crystal surface.

If the polymer functional group being monitored for dilation is relatively dilute (high molecular weight of repeat unit) and can be considered a weak absorber, then one may assume a linear relationship between the IR absorbance of a polymer peak and the polymer dilation, which leads to

$$\frac{\Delta V}{V_0} = -\frac{\Delta A}{A_0} \tag{8}$$

where ΔA and ΔV represent the changes in IR absorbance and sample volume, respectively, relative to their initial values, A_0 and V_0. Since the carbonyl group used to follow dilation in this study is neither dilute nor weak, the validity of using eq 8 certainly comes into question. Although eq 5 strictly applies to weak IR absorption, the ratio of absorbances in eq 8 can be used to approximate the ratio of carbonyl group concentrations provided ratios of the extinction coefficients and depths of penetration are not far from unity. If eq 8 were applied to a system in which the change in IR absorbance, ΔA, was large, then the difficulties associated with a strong IR absorber, points (a) and (b) above, would complicate the analysis. The extinction coefficient and depth of penetration can no longer be treated as constants in this case, and linearity between absorption and concentration (and hence dilation) would not hold. However, over relatively small changes in concentration, even those that occur at high concentrations with strong absorbers, linear approximations can be made. In this work, the extent of swelling is low (less than 10%), leading to relatively small changes in the measured absorbances of the carbonyl group (Figure 4). Therefore, eq 8 should be valid for measuring dilation in the polymers studied here. Direct observation of dilation using a CCD camera is included in this study to test the suitability of ATR spectroscopy with eq 8 for monitoring dilation under these conditions.

In data analysis, the complete thermoelastodiffusivity problem for the polymer−penetrant system should be addressed. In the present work, however, the dilation process and the different experimental conditions are described through a simplified, uncoupled, isothermal theory for which temperature effects and diffusivity changes due to elastic deformation are both neglected.

Moreover, under linear elasticity conditions the total strain can be expressed by the principle of superposition:

$$\epsilon = \epsilon^{\mathrm{M}} + \epsilon^{\mathrm{D}} \tag{9}$$

where ϵ^{M} is the contribution from the mechanical forces and ϵ^{D} is the one from the stress-free diffusion-induced strains. With this assumption, considering an isotropic material, each element $\epsilon_{ij}^{\mathrm{D}}$ of ϵ^{D} may be written in the form

$$\epsilon_{ij}^{\mathrm{D}} = \beta(C)\delta_{ij} \tag{10}$$

where β is a swelling function dependent on the actual penetrant concentration in the polymeric matrix and δ_{ij} is the Kronecker delta.

The elements of the mechanical stress tensor $\boldsymbol{\sigma}$ are defined by the relation

$$\sigma_{ij} = E_{ijlm}\epsilon_{lm}^{\mathrm{M}} = E_{ijlm}(\epsilon_{lm} - \beta(C)\delta_{lm}) \tag{11}$$

where E_{ijlm} belongs to a fourth-order elastic tensor. By considering the symmetry of both the stress and the strain tensor and the isotropy of the materials, no shear effects are present, and eq 11 can be simplified to the more common relationship

$$\boldsymbol{\sigma} = \mathbf{E}(\boldsymbol{\epsilon} - \boldsymbol{\beta}(C)) \tag{12}$$

where $\boldsymbol{\sigma}$ and $\boldsymbol{\epsilon}$ are vectors, $\mathbf{E}$ is a second-order tensor, and

$$\boldsymbol{\beta} = \{\beta_i(C)\} = \begin{cases} \beta(C), & i \le 3 \\ 0, & i > 3 \end{cases}$$

Considering that the two experimental methods involve different mechanical conditions, a free sample for the CCD camera experiment and a sample with a supported face in the ATR experiments where only the out-of-plane deformation is allowed, two different solutions result from these equations. In the first case, the dilation is only due to the diffusion process, and no external mechanical forces are considered, $\boldsymbol{\sigma} = 0$. Therefore, eq 12 leads to

$$\boldsymbol{\epsilon} = \boldsymbol{\beta}(C) \tag{13}$$

In this first-order theory, the overall volumetric change can be expressed by

$$\frac{\Delta V}{V_0} = \epsilon_{xx} + \epsilon_{yy} + \epsilon_{zz} = 3\epsilon_{xx} = 3\beta(C) \tag{14}$$

The boundary conditions for the supported film are quite different. Neglecting the boundary effects, the in-plane strain is prevented, and only the out-of-plane mechanical stress is reasonably null:

$$\sigma_{zz} = 0, \quad \epsilon_{xx} = 0, \quad \epsilon_{yy} = 0 \tag{15}$$

With these constraints, the relative volume change of the polymer during sorption is the out-of-plane

deformation (ϵ_{zz}) that can be calculated from eqs 9 and 12, leading to the following solution:

$$\epsilon_{zz} = \left(\frac{2\nu}{1-\nu} + 1\right)\beta(C)$$

$$\sigma_{xx} = \sigma_{yy} = -\frac{E}{1-\nu}\beta(C) \tag{16}$$

where E is Young's modulus and ν is the Poisson ratio.

Experimentally, it is well-known that ν for rubbery polymers is close to the ideal value of 0.5, whereas for glassy polymers, it can vary from 0.35 to 0.47. To compare the two types of data (CCD and ATR), the factor $2\nu/(1-\nu)+1$ must be evaluated for the three polymers used in this study. Since PEUT and PVAc are rubbery systems at 40 °C, a value of 0.5 was used for the Poisson ratio in both cases; for PC, the value reported by the supplier, $\nu = 0.45$, was used. Taking these values into account, the dilation data for PC, obtained with the ATR technique and analyzed with eq 16, was increased by a factor 1.15 to be properly compared with the corresponding data for the free sample.

Thermodynamic Models

In the present work, thermodynamic models were considered with the aim of testing the possibility of obtaining reliable information on polymer swelling from solubility data. Considering the substantial differences in the systems under consideration, two models were applied: the lattice fluid model, developed by Sanchez and Lacombe (SL) in 1976,[31,32] which has proved to be particularly suitable in describing equilibrium polymer−penetrant systems, and the nonequilibrium lattice fluid model (NELF) developed from Doghieri and Sarti,[33,34] which represents an extension of the previous theory to systems characterized by a certain departure from equilibrium, as is the case of sorption in glassy polymers. Both models can predict polymer dilation from the sorption isotherm and have been widely described in the literature, so only the major results will be reported here.

The SL model treats the material as a lattice on which molecules or atoms of different species can be placed. Statistical analysis of the possible combinations of molecules on the lattice and evaluation of the energetic interaction between adjacent, occupied sites leads to an expression for the entropy and internal energy of the system from which an equation of state can be built for the compound or mixture under consideration. The resulting relationship for a pure component is

$$\rho_1 = \rho_1^*\left\{1 - \exp\left[-\left(\frac{\rho_1}{\rho_1^*}\right)^2\frac{T_1^*}{T} - \frac{T_1^* p}{T P_1^*} - \left(\frac{\rho_1}{\rho_1^*} - \frac{R T_1^*}{M_1 P_1^*}\rho_1\right)\right]\right\} \tag{17}$$

and can be written specifically for a polymer−penetrant mixture as

$$\rho = \rho^*\left\{1 - \exp\left[-\left(\frac{\rho}{\rho^*}\right)^2\frac{T^*}{T} - \frac{T^* p}{T P^*} - \left(\frac{\rho}{\rho^*} - \frac{R T^*}{M_1 P^*}\omega_1\rho\right)\right]\right\} \tag{18}$$

In these equations T, p, and ρ represent the actual temperature pressure and density of the system, R is the ideal gas constant, ω_1 is the penetrant mass fraction in the mixture, and T^*, P^*, and ρ^* are the characteristic parameters of the model that refer to the system properties in the hypothetical liquid phase at 0 K.

For pure components, these parameters must be fitted to experimental data to make the model completely operative. In the case of a mixture, they can be calculated from those of the pure substances through simple mixing rules that, for a binary mixture, can be written as

$$\frac{1}{\rho^*} = \frac{\omega_1}{\rho_1^*} + \frac{\omega_2}{\rho_2^*}$$

$$P^* = \rho^*\left(\frac{P_1^*\omega_1}{\rho_1^*} + \frac{P_2^*\omega_2}{\rho_2^*} + \frac{\omega_1\omega_2}{\rho_2^*\,\rho_1^*}\rho^*\Delta P_{12}^*\right)$$

$$T^* = \frac{P^*}{\rho^*\left(\dfrac{P_1^*\omega_1}{T_1^*\,\rho_1^*} + \dfrac{P_2^*\omega_2}{\rho_1^*\,T_2^*}\right)} \tag{19}$$

The only additional parameter that must be regressed from mixture experimental data is ΔP_{12}^*. Once all of these parameters are known, the evaluation of the mixture composition and density at a given pressure can be easily obtained by equating the chemical potential of the penetrant (subscript 1) in the polymeric and vapor phases as follows:

$$\ln\left(\frac{\omega_1\rho^*}{\rho_1^*}\right) + \left(1 - \frac{\omega_1\rho^*}{\rho_1^*}\right) + \frac{\rho M_1\Delta P_{12}^*}{R T\rho^*\rho_1^*}\left(1 - \frac{\omega_1\rho^*}{\rho_1^*}\right)^2 + \frac{M_1 P^*}{R T^*\rho_1^*}\left[-\frac{\rho T^*}{T\rho^*} + \frac{T^*\rho^* p}{T\rho P^*} - \left(1 - \frac{\rho^*}{\rho}\right)\ln\left(1 - \frac{\rho}{\rho^*}\right)\right] + \ln\left(\frac{\rho}{\rho^*}\right) = \frac{M_1 P_1^*}{R T_1^*\,\rho_1^*}\left[-\frac{\rho_1 T_1^*}{T\rho_1^*} + \frac{T_1^*\,\rho_1^* p}{T\rho_1 P_1^*} - \left(1 - \frac{\rho_1^*}{\rho_1}\right)\ln\left(1 - \frac{\rho_1}{\rho_1^*}\right)\right] + \ln\left(\frac{\rho_1}{\rho_1^*}\right) \tag{20}$$

The expression on the left-hand side of eq 20 is the penetrant chemical potential in the polymeric mixture, while that on the right-hand side is the chemical potential of the pure vapor.

The NELF model is based on the assumption that a suitable parameter to account for the departure from equilibrium in a glassy polymer can be found in its density, which at a given temperature and pressure is different than the one at equilibrium. From this assumption and assuming that the system rheology can be described by the Voigt model, any equilibrium expression for the Helmoltz free energy, as a function of temperature, volume, and composition, can be extended to the nonequilibrium domain by simply replacing the density of the polymeric species with its nonequilibrium value observed in the actual state of the system. Once such an expression is available, the other properties of the glassy state can be calculated from the relationships of classical thermodynamics, with the exception of the P−V−T equation of state.

In the NELF development in particular, the Helmoltz free energy expression obtained by the Sanchez−Lacombe model is properly used to obtain a new expression

Table 2. Characteristic Pure-Component Parameters for SL and NELF Models

	p^* (MPa)	T^* (K)	ρ^* (g/cm^{-3})	ref
PC	534	755	1.275	33
PVAc	510	592	1.284	33
PEUT	450	550	1.132	this work
CH_3CN	910	505	0.855	this work

for the solvent chemical potential in the glassy polymer−penetrant mixture. This allows one to calculate the penetrant concentration in the mixture once the pressure, temperature, and nonequilibrium polymer density are known. To that aim, the chemical potential of the solvent in the pure vapor phase as reported on the right-hand side of eq 20 must be equated to the chemical potential of the penetrant in the glassy phase, $\mu_1^{(G)}$, which can be written as

$$\mu_1^{(G)} = RT\left\{\ln\left(\frac{\omega_1\rho_2}{\omega_2\rho_1^*}\right) - \frac{M_1P_1^*}{\rho_1^*RT_1^*} \times \left\{\left[1 + \left(\frac{T_1^*P^*}{T^*P_1^*} - 1\right)\frac{\omega_2\rho^*}{\rho_2}\right]\ln\left(1 - \frac{\rho_2}{\omega_2\rho^*}\right) + \frac{T_1^*P^*}{T^*P_1^*} + \frac{\rho_2}{\omega_2\rho^*}\left[\frac{T_1^*}{T}\left(1 + \frac{P^*}{P_1^*} - \left(\omega_2\frac{\rho^*}{\rho_2^*}\right)^2\frac{\Delta P_{12}^*}{P_1^*}\right)\right]\right\} + 1\right\} \quad (21)$$

where the subscripts 1 and 2 refer to penetrant and polymer, respectively. The definitions of the various terms in eq 21 are the same as in the SL model, of which the NELF model is an extension. Polymer density cannot be calculated from the equation of state given by eq 18, but must be obtained independently. In particular, it has been shown that, for many glassy polymers, the density can be assumed to be proportional to the pressure of the vapor phase:[34]

$$\rho_2(p) = \rho_2^0(1 - kp) \quad (22)$$

where ρ_2^0 represents the dry polymer density, k is a swelling coefficient, and both contribute to the determination of the nonequilibrium density in swollen systems.

Pure component characteristic parameters for this study were either found in the literature or calculated from PVT data and are reported in Table 2. The binary parameter ΔP_{12}^* was treated in all cases as a fitting parameter. For the sake of convenience it was written as

$$\Delta P_{12}^* = P_1^* + P_2^* - 2\psi\sqrt{P_1^*P_2^*} \quad (23)$$

where ψ represents the dimensionless binary parameter, whose first-order approximation was suggested by Sanchez and Lacombe as $\psi = 1$. Regression on experimental data was performed by adjusting ψ to minimize the square mean error between the data and the model prediction. This parameter does not deviate significantly from unity, so it is particularly useful as a fitting parameter. The values obtained for the different systems in this study are reported in Table 3. One additional assumption was made for the PC−CH_3CN system. In this case, the value of the binary parameter was fitted together with the swelling coefficient k to correlate the data (see Table 3).

Table 3. Binary Parameters from Model Regressions

	Ψ	k (MPa^{-1})
PC	1.028	6.22
PVAc	0.983	
PEUT	0.974	

Results and Discussion

Solubility. The problems associated with the experimental measurement of volume change during sorption make the prediction of polymer swelling from solubility data very appealing. Generally speaking, solubility data are more reliable and readily available for a large number of systems under a wide range of experimental conditions. Sorption isotherms were measured and are reported in Figure 5 for all of the polymers considered here. PVAc and PEUT show an upward curvature typical of rubbery polymers, whereas PC presents an opposite behavior with a single downward concavity in the isotherm. PEUT, among the three polymers, exhibits the lowest affinity for acetonitrile, while PC has the highest solubility at low activities (ratio between the experimental pressure and the penetrant vapor pressure at the experimental temperature). PVAc has the highest value of penetrant content at the higher activities, reaching a mass uptake of 10% at activity 0.5. This value is rather high and indicates a strong affinity between the diffusing substance and this polymer. In fact, PVAc completely dissolves when immersed in liquid acetonitrile. In Figure 5 the model regressions for the different systems are also shown. As previously mentioned, the SL model was used to describe the solubility data of PEUT and PVAc, and the NELF model was used in the case of PC. The model regressions are very satisfactory, and relative errors for the different systems seldom exceed 10%.

As far as the glassy polymer is concerned, it is worthwhile to recall that in the regression only two adjustable parameters were considered, with the dry polymer density fixed to the value reported by the supplier. It should be noted, however, that the NELF model is extremely sensitive to this parameter, and a minimal change in its value can cause a dramatic variation in other quantities, such as the swelling coefficient k. This fact is of great interest considering that, during the preparation of separation membranes, a slight change in the polymer density can occur quite

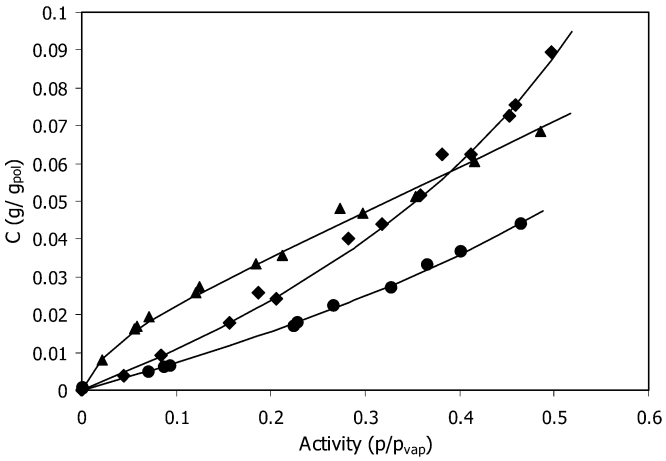

Figure 5. Experimental sorption isotherms and model regressions for acetonitrile in PVAc (diamonds), PEUT (circles), and PC (triangles). Parameters used for regression are in Table 2.

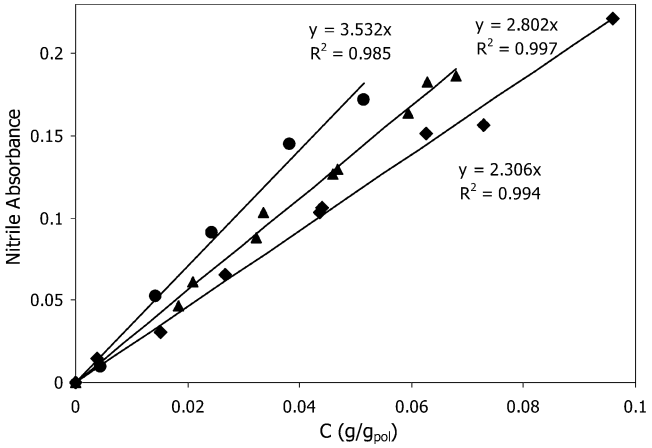

Figure 6. Correlation between IR absorbance and acetonitrile concentration in PVAc (diamonds), PEUT (circles), and PC (triangles).

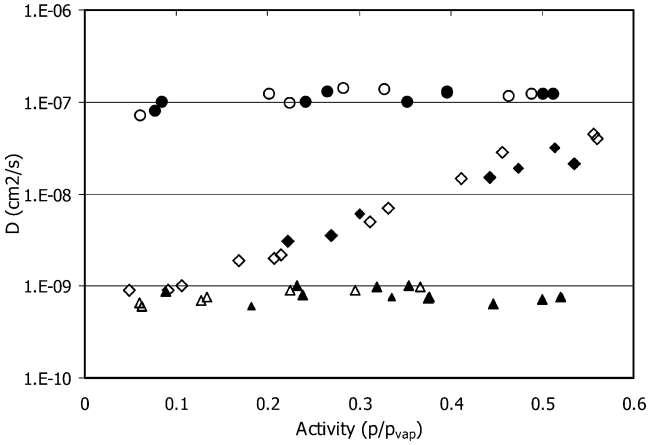

Figure 7. Effective diffusion coefficient of acetonitrile in PEUT (circles), PVAc (diamonds), and PC (triangles). Open symbols refer to gravimetric data whereas solid ones refer to ATR experiments.

easily. For this reason, a three-parameter fitting procedure was considered for the system PC−CH_3CN, naturally leading to a better fit, with only a variation of a few percent in the dry polymer density. This fact is reported here for completeness and will be discussed below in the analysis of the dilation data.

The data analyzed in this section were obtained using the quartz spring apparatuses since FTIR-ATR spectroscopy does not give directly the solubility of the penetrant, but only the infrared absorbance of a peak associated with the penetrant in the polymer. To obtain the equilibrium penetrant concentration in the polymer, a calibration is required. The results obtained were in accordance with the Beer−Lambert law reported in eq 5, whose expression for the equilibrium concentration can be written as

$$A = \epsilon^* CL \tag{24}$$

The linearity of the A−C plot, presented in Figure 6, allows one to conclude that solubility, as calculated from the ATR experiments, is consistent with the gravimetric data. Moreover, since the constancy of the molar extinction coefficient assumed in eqs 5 and 7 is verified, the diffusion coefficient can be evaluated from these data as described above.

Diffusion Data. The effective diffusion coefficients of acetonitrile in the different systems considered were obtained through the ATR technique, using eq 4, as well as through the gravimetric technique, from eq 7, and are shown in Figure 7. Acetonitrile diffusion in the three polymers was Fickian in nature. Very slight deviations from theoretical Fickian behavior were encountered during data analysis, possibly the result of the dependence of the diffusion coefficient on the penetrant concentration in the polymer. This dependence is particularly evident in the case of PVAc, in which the acetonitrile diffusion coefficient increases roughly 2 orders of magnitude (from 9×10^{-10} to 5×10^{-8} cm^2/s) when the penetrant activity rises from 0.1 to 0.5. Both PC and PEUT are instead characterized by nearly constant diffusion coefficients of approximately 1×10^{-9} for the former and 1×10^{-7} for the latter.

The reason for the different behavior in PVAc with respect to the other two polymers can be attributed to the previously mentioned affinity between this polymer and acetonitrile. This penetrant not only completely dissolves PVAc at activity one but highly increases the polymer chain mobility at moderate activities. The films used for the gravimetric experiments, in fact, lost their dimensional stability during sorption. The reason for this behavior can be easily surmised from the characteristic features of PVAc. Films of this polymer are obtained at room temperature, just below its T_g, and experiments are performed a few degrees above T_g. Since solvent evaporation is relatively fast, some stresses may remain frozen in the film, which completely relax only once T_g is depressed by the sorption process, leading to shrinkage and shape rearrangement. It is interesting to note that the diffusion coefficient of acetonitrile in PVAc increases from a value that is typical of a glassy polymer, such as PC, to that obtained for a rubber well above its T_g, as in the case of PEUT.

One point that deserves to be emphasized is the good agreement between the diffusion results obtained with both techniques. Other studies in the literature have compared results from these two methods for a rubbery polymer, where the gravimetric technique was used primarily to test the reliability of ATR data.[13] The results here extend the comparison to glassy polymers. This is not trivial as newly cast films are required for each ATR experiment, which can be critical for systems endowed with memory, such as glassy polymers.

Dilation Data. Figures 8 and 9 show dilation data for the two rubbery polymers and the glassy polymer, respectively. The relative volume change is plotted against the penetrant activity, and the data from both experimental techniques are reported. The agreement in the results is generally very good and confirms not only the potential of the ATR technique for the measurement of polymer swelling during sorption but also the original hypothesis of isotropic dilation and linear elasticity used for calculation and data analysis. In the case of PVAc, only one low activity point was obtained through the CCD system owing to the excessive softening of the sample at moderate activities. However, this one point appears consistent with the experimental ATR data for this polymer. The increased chain mobility induced by acetonitrile sorption in PVAC results in a dilation of the polymer matrix of approximately 10% at activity 0.5, roughly double the corresponding values for PC and PEUT at the same experimental conditions.

PC and PEUT exhibit very similar dilation behaviors despite their different thermodynamic states. For PC, the volume changes upon sorption are only slightly

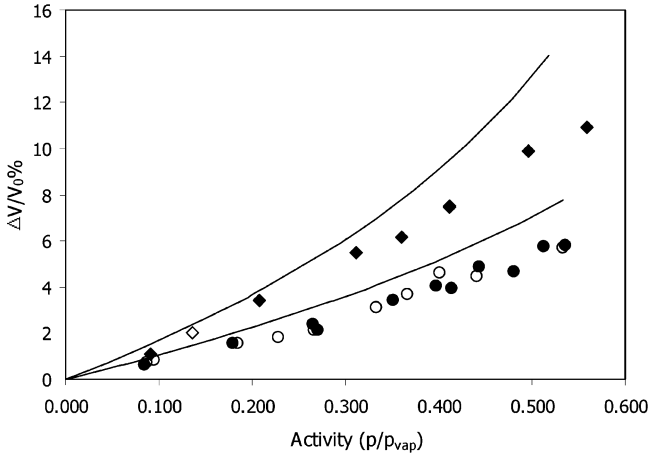

Figure 8. Comparison between ATR (solid) and CCD (open) dilation data for the two rubbery systems, PVAc (diamonds) and PEUT (circles). The solid line represents SL model prediction with the parameters used for regressing the sorption isotherm.

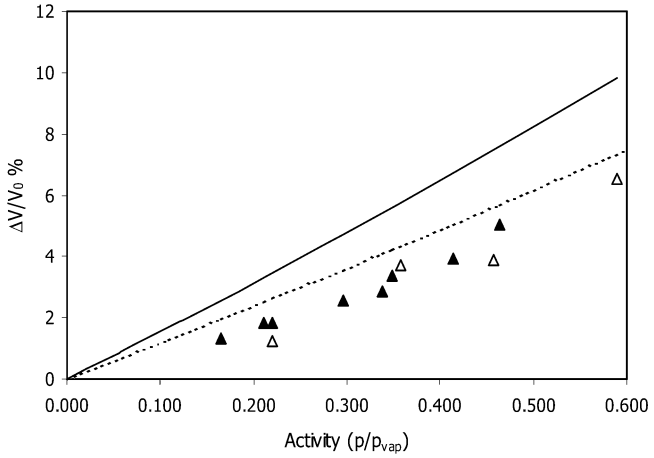

Figure 9. Comparison between ATR (solid) and CCD (open) dilation data for the glassy system, PC. The solid line represents NELF model prediction with the parameters reported in Table 2. The dashed line is a correlation with initial density as a fitting parameter (regression made on sorption data).

lower than those for PEUT at the same activity. However, a comparison between the data for these two polymer can be somewhat misleading because quite different values of penetrant concentration exist in the two polymers at the same value of chemical potential in the vapor phase. A different interpretation of the dilation data can be obtained by considering function $\beta(C)$ introduced in eq 10 and comparing the volume change vs the penetrant concentration. Vapor activity can be linked to the actual penetrant concentration by fitting the experimental data presented in Figure 5. Since the agreement between experimental points and model correlation is very good, no significant error is introduced. Results are shown in Figure 10. In this figure, it is easy to distinguish the different effects that the penetrant has on the polymeric matrix for the rubbery polymer compared to the glassy polymer. The PC dilation vs concentration isotherm shows a clear upward curvature while that for PEUT or PVAc increases linearly with penetrant content in the polymer, being slightly higher in the latter.

The difference in dilation behavior as a function of penetrant concentration between the rubbery and glassy

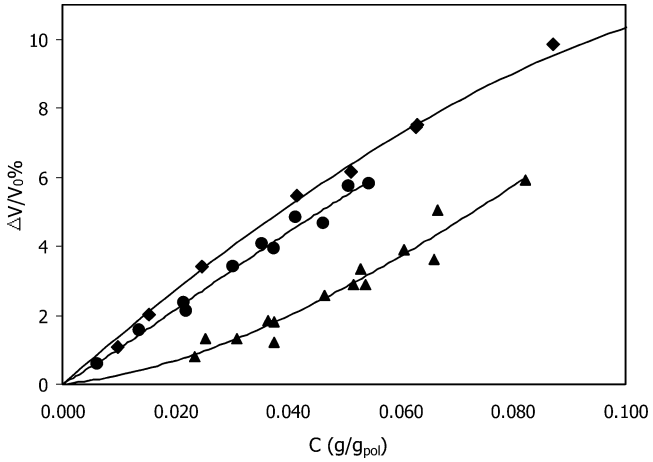

Figure 10. Relationship between volumetric change and acetonitrile concentration in PVAc (diamonds), PEUT (circles), and PC (triangles).

polymers is related to the different mobilities of the polymer chains as a consequence of the thermodynamic state of the system. The glassy polymer shows a lower capacity of chain relaxation to accommodate the incoming penetrant, requiring higher penetrant contents to realize the same volume dilation. Similar conclusions were drawn by Barbari,[35] who described penetrant-induced dilation in glassy polymers considering that only a portion of the diffusing molecules actively participate in swelling the polymer while the others sorb into the matrix microvoids without contributing to the system dilation. The rubbery polymer−penetrant systems behave as pseudo-liquid mixtures, in which the dilation is directly related to the ideality of the system and to the partial molar volume of the penetrant in the mixture. The partial molar volume is related to the slope of $\beta(C)$ and is nearly constant in the case of PEUT ($\approx$ 43 cm^3/mol) and at low concentrations in PVAc ($\approx$ 42 cm^3/mol). When mass uptake exceeds 6% in PVAc, the acetonitrile partial molar volume appears to decrease, but it is worth pointing out again that the ATR data cannot be further verified through CCD camera observation, and this tendency may be the result of measurement errors. For glassy PC, the penetrant partial molar volume has a less intuitive physical meaning than in the rubbery polymers, particularly at low concentrations when nonswelling sorption is occurring; it increases with solvent concentration, approaching a value typical of rubbery polymers as the T_g is depressed by the penetrant.

The different volumetric behaviors of glassy and rubbery polymers during sorption become even more evident when the kinetic dilation data are considered. The use of FTIR-ATR spectroscopy allows one to obtain, simultaneously, data for penetrant diffusion and polymer swelling by monitoring integrated absorbances of penetrant and polymer peaks, respectively. It is thus possible to understand how these two kinetic processes are related. In Figure 11, polymer (C═O) vs penetrant (C≡N) IR absorbances are plotted for the three polymers. It is clear that PC exhibits very different behavior relative to the other polymers. For PEUT and PVAc, there is a linear correlation between the dilation and concentration data, whereas for the glassy PC, there is a downward curvature that reveals a delay in swelling with respect to the diffusion process. For the rubbery polymers, the experimental results can be easily explained by considering that the chain mobility in rub-

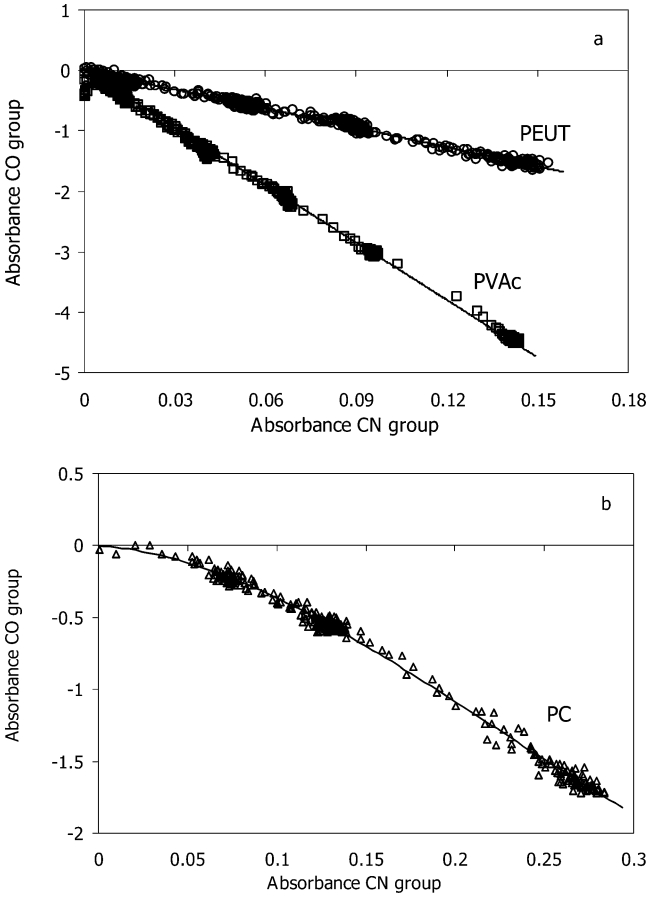

Figure 11. Kinetics of dilation: comparison between carbonyl absorbance (polymer) and nitrile absorbance (penetrant). For the two rubbery systems (a), there is a linear correlation whereas for the glassy polymer (b), a delay in swelling is evident.

bers is high enough to instantaneously reorder to accommodate the incoming penetrant. As a consequence, during the dynamic part of the sorption process, local equilibrium between the penetrant molecules and the surrounding matrix exists, such that the solvent throughout the system has the same partial molar volume that it would have in a fully equilibrated mixture. Therefore, since the partial molar volume is relatively constant in the rubbery polymers, a linear relationship is observed between the volume change and the penetrant concentration.

The results for PC are substantially different. It is well-known that glassy polymers can exhibit different diffusion behaviors depending on how the matrix reacts to the presence of penetrant. The existence of case II, Fickian, or anomalous diffusion is typically related to the rate of matrix relaxation with respect to that of penetrant diffusion. In the present case, however, it does not appear that the swelling delay is due to a different response time of the polymer matrix to penetrant sorption. The plateau in Figure 11b is, in fact, present only in the integral sorption run and in the first step of differential experiments, as if it were directly related not only to the structure of the polymer but also to the amount of penetrant already inside the matrix. It appears as if the first molecules entering the polymer move inside the free volume of the matrix without contributing to polymer swelling, and then only after most of the microvoids are filled does swelling take place. During the early stages of sorption, the polymer seems to behave as a rigid matrix, swelling is negligible, and the penetrant diffuses mainly in the holes of the polymer lattice. Then, the chains start to relax and the behavior progressively changes to a linear function between dilation and penetrant content. The concept of diffusion in an unrelaxed matrix is usually considered for glassy polymers with very high fractional free volumes,[36] but for very low penetrant concentrations, it could be extended to other glassy polymers. In this case, the polymer does not dilate at C≡N absorbance values less than approximately 0.05, which from the calibration curve presented in Figure 6 corresponds to a weight fraction less than 2%.

Concluding the analysis of the volumetric data, it is worthwhile to consider the prediction of polymer swelling from the thermodynamic models presented here. In Figures 8 and 9, the dilation isotherms as predicted from the SL and NELF models for the rubbery and glassy polymers, respectively, are given by the solid lines. The characteristic parameters listed in Table 2 and obtained from fitting the sorption isotherms were used in this calculation. No additional adjustable parameters were considered, and the two models are used in a completely predictive manner. In each case, the model prediction overestimates the experimental dilation data, but the amount of error is different. For PEUT, the differences between the experimental data and the model results are minor, and their agreement can be considered satisfactory considering the fact that the SL model is used without any adjustable parameter. For PVAc and PC, the errors are rather high, and it is worthwhile to consider these systems in more detail to explain the deviations.

For the PVAc−acetonitrile system, the dilation data seem to be in fairly good agreement with the model prediction at activity values less than 0.4, where the errors between experimental data and SL model predictions are similar to those obtained for the other rubbery system. The previously mentioned problems with dimensional stability and softening of the PVAc prevents the drawing of any reasonable and reliable conclusions at higher activities, since no gravimetric data could be collected in this range to check the ATR response.

In the case of PC, the experimental data from the two techniques compare well and are available at all activities. The large deviation from the model prediction may be due to the extreme sensitivity of the NELF model to the value of the dry polymer density in the description of the sorption isotherm. This parameter was fixed at the value reported by the supplier during the fitting procedure, but it is processing dependent and can change as a result of the casting procedure. If a regression is made with this parameter as freely adjustable, the NELF model allows a satisfactory representation of the data, improving the description of both sorption and dilation isotherms (errors are reduced by a half) with a small change in the dry polymer density (less than 4%). The resulting regression is shown as a dotted line in Figure 9. This regression, however, may not reflect the actual state of the polymer during sorption but is reported here to demonstrate the internal consistency of the NELF model in representing both sorption and dilation behaviors in the system.

Conclusion

In the present work, time-resolved ATR−FTIR spectroscopy was used to study acetonitrile diffusion in three

polymers and the volumetric behavior of the polymeric matrices upon sorption. The choice of polymers (PVAc, PC, and PEUT) was made because of their practical importance in sensor development and because their infrared spectral characteristics made them particularly suitable for ATR analysis. The ATR results were compared with measurements made independently with a quartz spring apparatus, for solubility and diffusivity data, and with a CCD camera for swelling. Two thermodynamic models (SL and NELF), suitable for the analysis of sorption and dilation of rubbery and glassy polymers, respectively, were considered to test whether dilation can be predicted from solubility data.

The experimental data obtained through the ATR technique were in very good agreement with the corresponding measurements made with the other experimental methods. In particular, it should be stressed that the need for newly cast samples in each ATR experiment did not appear to have any influence on the experimental results for the glassy polymer, PC. For the first time, to our knowledge, the ATR technique has been used to obtain quantitative information on polymer swelling upon sorption, representing another application of this novel technique to the study of mass transport in polymeric systems. In general, the thermodynamic models overestimate the experimental data; however, a fairly good prediction of the polymer dilation during sorption was obtained for the rubbers with the SL model. More critical is the situation in the case of the glassy polymer owing to the difficulties inherent in modeling nonequilibrium systems. However, the NELF model did reasonably well in calculating both sorption and dilation data with only three adjustable parameters.

Acknowledgment. This work was partially supported by the Italian Ministry of Education and University (PRIN 2001 ex 40%). We gratefully acknowledge the support of the University of Bologna and Johns Hopkins University (JHU), which made possible the visiting research appointment of Marco Giacinti B. in the Department of Chemical Engineering at JHU.

References and Notes

(1) Mirabella, F. M. *J. Polym. Sci., Polym. Phys. Ed.* **1984**, *22*, 1283.
(2) Mirabella, F. M. *J. Polym. Sci., Polym. Phys. Ed.* **1984**, *22*, 1293.
(3) Yuan, P.; Sung, C. S. P. *Macromolecules* **1991**, *24*, 6095.
(4) Huang, J.; Urban, M. W. *Appl. Spectrosc.* **1993**, *47*, 973.
(5) Ekgasit, S.; Ishida, H. *Appl. Spectrosc.* **1997**, *51*, 461.
(6) Van Alsten, J. G.; Lustig, S. R. *Macromolecules* **1992**, *25*, 5069.
(7) Jabbari, E.; Peppas, N. A. *Macromolecules* **1993**, *26*, 2175.
(8) Jabbari, E.; Peppas, N. A. *J. Mater. Sci.* **1994**, *29*, 3969.
(9) Xu, J. R.; Balik, C. M. *Appl. Spectrosc.* **1988**, *42*, 1543.
(10) Schlotter, N. E.; Furlan, P. Y. *Vibr. Spectrosc.* **1992**, *3*, 147.
(11) Fieldson, G. T.; Barbari, T. A. *Polymer* **1993**, *34*, 1146.
(12) Fieldson, G. T.; Barbari, T. A. *AIChE J.* **1995**, *41*, 795.
(13) Hong, S. U.; Barbari, T. A.; Sloan, J. M. *J. Polym. Sci., Polym. Phys. Ed.* **1997**, *35*, 1261.
(14) Balik, C. M.; Simendinger, W. H. An. *Polymer* **1998**, *39*, 4723.
(15) Rajagopalan, G.; Immordino, K. M.; Gillespie, J. W.; McKnight, S. H. *Polymer* **2000**, *41*, 2591.
(16) Van Alsten, J. G.; Colburn, J. C. *Macromolecules* **1994**, *27*, 3746.
(17) Sammon, C.; Mura, C.; Yarwood, J.; et al. *J. Phys. Chem. B* **1998**, *102*, 3402.
(18) Yarwood, J.; Sammon, C.; Mura, C.; Pereira, M. *J. Mol. Liq.* **1999**, *80*, 93.
(19) Elabd, Y. A.; Barbari, T. A.; Sloan, J. *Polymer* **2000**, *41*, 2203.
(20) Elabd, Y. A.; Barbari, T. A. *AIChE J.* **2002**, *48*, 1610.
(21) Hong, S. U.; Barbari, T. A.; Sloan, J. M. *J. Polym. Sci., Polym. Phys. Ed.* **1998**, *36*, 337.
(22) Cornilia, C.; Noetzel, G.; Weimar, U.; Goepel, W. *Sens. Actuators B* **1995**, *24*−*25*, 357.
(23) Schierbaum, K. D.; Gerlach, A.; Hang, M.; Goepel, W. *Sens. Actuators A* **1992**, *31*, 130.
(24) Hang, M.; Schierbaum, K. D.; Endres, H. E.; Drost, S.; Goepel, W. *Sens. Actuators A* **1992**, *32*, 326.
(25) Balik, C. M.; Xu, J. R. *J. Appl. Polym. Sci.* **1994**, *52*, 975.
(26) Sammon, C.; Yarwood, J.; Everall, N. *Polymer* **2000**, *41*, 2521.
(27) Jamroz, D.; Stangret, J.; Lingdren, J. *J. Am. Chem. Soc.* **1993**, *115*, 6165.
(28) Takamuku, T.; Tabata, M.; Yamaguchi, A.; Nishimoto, J.; Kumamoto, M.; Wakita, H.; Yamaguchi, T. *J. Phys. Chem. B* **1998**, *102*, 8880.
(29) Crank, J.; Park, J. S. In *Diffusion in Polymers*; Academic Press: New York, 1968.
(30) Huang, J. B.; Urban, M. W. *Appl. Spectrosc.* **1992**, *46*, 1014.
(31) Lacombe, R. H.; Sanchez, I. C. *J. Phys. Chem.* **1976**, *80*, 2568.
(32) Sanchez, I. C.; Lacombe, R. H. *J. Phys. Chem.* **1976**, *80*, 2352.
(33) Doghieri, F.; Sarti, G. C. *Macromolacules* **1996**, *29*, 7885.
(34) Giacinti Baschetti, M.; Doghieri, F.; Sarti, G. C. *Ind. Eng. Chem. Res.* **2001**, *40*, 3027.
(35) Barbari, T. A. *J. Polym. Sci., Part B: Polym. Phys.* **1993**, *31*, 501.
(36) Doghieri, F.; Biavati, D.; Sarti, G. C. *Ind. Eng. Chem. Res.* **1996**, *35*, 2420.
(37) Harrick, N. J. *Opt. Soc. Am.* **1965**, *55*, 851.

MA0302457